Journal of Medicinal Chemistry Article

J. Med. Chem. **2009,** *52,* 4683–4693 **4683**
DOI: 10.1021/jm9001499

3,5-Diphenylpent-2-enoic Acids as Allosteric Activators of the Protein Kinase PDK1: Structure−Activity Relationships and Thermodynamic Characterization of Binding as Paradigms for PIF-Binding Pocket-Targeting Compounds†

Adriana Stroba,‡ Francis Schaeffer,§ Valerie Hindie,∥ Laura Lopez-Garcia,∥ Iris Adrian,∥ Wolfgang Fröhner,‡ Rolf W. Hartmann,‡ Ricardo M. Biondi,∥ and Matthias Engel*,‡

‡*Pharmaceutical and Medicinal Chemistry, Saarland University, P.O. Box 151150, D-66041 Saarbrücken, Germany,* §*Unité de Biochimie Structurale (CNRS-URA 2185), Institut Pasteur, F-75724 Paris, France, and* ∥ *Department of Internal Medicine I, University of Frankfurt, Theodor-Stern-Kai 7, D-60590 Frankfurt a.M., Germany*

Received February 5, 2009

The modulation of protein kinase activities by low molecular weight compounds is a major goal of current pharmaceutical developments. In this line, important efforts are directed to the development of drugs targeting the conserved ATP binding site. However, there is very little experience on targeting allosteric, regulatory sites, different from the ATP binding site, in protein kinases. Here we describe the synthesis, cell-free activation potency, and calorimetric binding analysis of 3,5-diphenylpent-2-enoic acids and derivatives as allosteric modulators of the phosphoinositide-dependent kinase-1 (PDK1) catalytic activity. Our SAR results combined with thermodynamic binding analyses revealed both favorable binding enthalpy and entropy and confirmed the PIF-binding pocket of PDK1 as a druggable site. In conclusion, we defined the minimal structural requirements for compounds to bind to the PIF-binding pocket and to act as allosteric modulators and identified two new lead structures (**12*Z*** and **13*Z***) with predominating binding enthalpy.

Introduction

Protein kinases are actively involved in the control and regulation of cellular processes. In addition, overexpression of protein kinases or loss of kinase regulatory mechanisms are observed in many human diseases such as cancer, inflammation, neurological (e.g., Alzheimer's disease), and metabolic disorders (e.g., type 2 diabetes). Thus, protein kinases are an important drug target class for the treatment of diverse human diseases.[1]

The phosphoinositide-dependent protein kinase 1 (PDK1[a]) is in the center of growth factor and insulin signaling and is a master kinase that phosphorylates the activation loop of several protein kinases from the AGC group, including all PKC, PKB (also termed AKT), S6K, RSK, and SGK isoforms.[2] PDK1 has gained importance as a potential therapeutic target for cancer because several of the substrate protein kinases, comprising S6K, RSK, and PKB, regulate processes that are essential to the tumor cell such as cell growth and survival.[2,3]

We have discovered an allosteric site on PDK1 (termed the PIF-binding pocket), distant from the ATP binding site, and suggested the site as a possible target for drugs.[4,5] Interestingly, an equivalent hydrophobic motif (HM) binding pocket regulatory site exists on other AGC kinases. Therefore, our research on PDK1 may open the field to drug developments on other kinases sharing a similar mechanism of regulation.[6]

The PIF-binding pocket of PDK1 is a hydrophobic surface pocket neighboring a putative phosphate coordination site and is located on the small lobe of the PDK1 catalytic domain.[4,7] Its physiological ligands are C-terminal regions of PDK1 substrates that utilize a considerably larger area for interaction than just the hydrophobic pocket. The PDK1 PIF-binding pocket serves two functions: first, it is a docking site for transient interactions with the substrate proteins via their C-terminal hydrophobic motif (HM), comprising the sequence Phe-Xaa-Xaa-Phe. Second, binding of the peptides increases the intrinsic catalytic activity of PDK1. Almost all substrates of PDK1, including S6K, SGK, RSK, and the atypical PKCs, require this docking interaction with the PDK1 PIF-binding pocket in order to become phosphorylated at the activation loop, which results in full activation of the substrate kinase.[5,6,8] As the only known exception, PKB does not require interaction with the PIF-binding pocket of PDK1.[5,9]

Several reports have described small molecule inhibitors of PDK1 that target the ATP binding site.[10−14] One such non-specific inhibitor, UCN-01 (7-hydroxystaurosporine), is in clinical trials.[15−18] While these compounds have shown anticancer activities *in vivo*, coinhibition of additional protein kinases increases the risk of dose-limiting off-target effects. In fact, most ATP competitive inhibitors show limited selectivity,[19,20] implying that certain protein kinases have not been considered as suitable for drug development, in particular protein kinases for which closely related isoforms exist.

As an alternative and as a complement to ATP binding site-directed compounds, there is increasing interest in the development of non-ATP competitive strategies for protein kinase drug developments.[21] Most interestingly, the characterization

†PDB code of **2Z** with PDK1: 3HRF.

*To whom correspondence should be addressed. Phone: +49 681 302 70312. Fax: +49 681 302 70308. E-mail: ma.engel@mx.uni-saarland.de. Web site: http://www.pharmmedchem.de.

[a] Abbreviations: HM, hydrophobic motif; HWE, Horner−Wadsworth−Emmons; wt, wild type; ITC, isothermal titration calorimetry; PDK1, phosphoinositide-dependent kinase-1.

Published on Web 07/17/2009

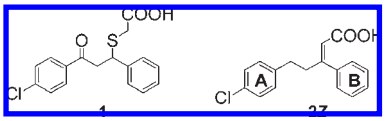

Figure 1. Hit compound (**1**) and new lead compound (**2*Z***).

of novel allosteric sites as druggable sites might enable the development of drugs with more subtle modulation of the protein kinase activity as compared to the complete inhibition of the enzymatic activity. For example, the targeting of allosteric-regulatory sites could potentially generate inhibitors but also protein kinase activating drugs. Recently, we have provided first evidence that a small molecule can trigger activation of PDK1.[22] Similarly, anacardic acid (6-pentadecatrienyl salicylic acid) was reported recently as an allosteric activator of Aurora A kinase.[23]

In the case of GPCRs, modulation of the receptor function by allosteric ligands has provided high selectivity and a far greater diversity in the repertoire of pharmacological effects can be achieved.[24] In the present report, we describe the design and synthesis of 3,5-diarylpent-2-enoic acids as novel PIF-binding pocket directed compounds and present SAR data on their allosteric activation potency. We provide the binding energetics of allosteric activators based on isothermal titration calorimetry, shedding light on relationships between structural properties, binding affinity, and allosteric activation. The general requirements for HM/PIF-binding pocket compounds are presented and discussed based on our recent cocrystallization of compound **2*Z*** with PDK1.[25]

Results and Discussion

1. Chemistry. In a previous report, we had published hit compound **1** as an activator of PDK1 (Figure 1). Drawbacks of this compound were the existence of a chiral center, yielding a racemic mixture with unknown contribution of each enantiomer to the total activity, and the sulfanyl moiety, which is prone to oxidations and potentially retro-Michael reactions. The design of the new structural analogues aimed at replacement of the chiral center by a double bond while retaining the combination of two sp^3 and one sp^2 hybridized C-atoms in the chain connecting the benzene rings, thus leading to compound **2*Z*** (Figure 1).

Syntheses of **2** and analogues **3**−**13** started with a Claisen−Schmitt condensation (method A) between acetophenone and a series of benzaldehydes **2d**−**13d** to obtain the chalcones **2c**−**13c** (Scheme 1). To selectively reduce the conjugated double bond of the chalcones, we utilized a convenient hydride transfer reaction (method B) from 3,5-bis(ethoxycarbonyl)- 1,4-dihydro-2,6-dimethylpyridine (HEH) catalyzed by silica gel,[26] which quantitatively afforded the saturated ketones **2b**−**13b**. Olefination of the carbonyl group in **2b**−**13b** was achieved by Horner−Wadsworth−Emmons reaction (HWE) (method C) with triethyl phosphonoacetate, yielding *E*/*Z*-mixtures of ethyl 3,5-diphenylpent-2-enoates (**2a**−**13a**, Scheme 1), which could be efficiently separated by flash column chromatography in all cases. We intentionally chose the reaction conditions to favor formation of both stereoisomers in order to isolate both compounds and test them separately. In the last step, the ethyl ester was hydrolyzed (method D) under basic conditions to yield the free 3,5-diphenylpent-2-enoic acids (**2*E***−**13*E***, **2*Z***−**13*Z***). For **2*E*** and **2*Z***, we determined the *E*/*Z* configuration exemplarily using 2D-NOESY−^{1}H NMR

Scheme 1. Synthesis of Compounds **2*E***−**13*E***, **2*Z***−**13*Z***, and **21*E***[a]

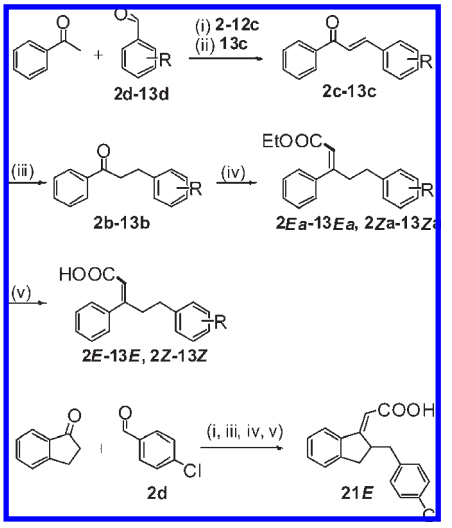

[a] Reagents and conditions: (i) method A: NaOH, EtOH, 1 h, rt; (ii) piperidine, EtOH, reflux, 16 h; (iii) method B: 3,5-bis(ethoxycarbonyl)-1,4-dihydro-2,6-dimethylpyridine, toluene, silica gel, 70 °C, 16 h; (iv) method C: triethyl phosphonoacetate, NaH, DME, 80 °C, 4 h; (v) method D: NaOH, EtOH, rt, 3 h. For substituents R, see Table 1.

Scheme 2. Synthesis of Compounds **14*E***, **14*Z***, and **15*E***[a]

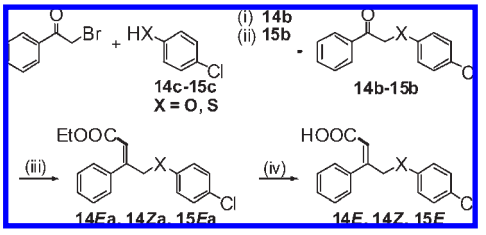

[a] Reagents and conditions: (i) K_2CO_3, EtOH, 80 °C, 1 h; (ii) 5% $BnNEt_3Cl$, 30% NaOH, CH_2Cl_2, rt, 16 h; (iii) method C: triethyl phosphonoacetate, NaH, DME, 80 °C, 4 h; (iv) method D: NaOH, EtOH, rt, 3 h.

(see Supporting Information). The *E*/*Z* assignment of the other compound pairs was done by comparison of the corresponding NMR spectra with those of ***2E*** and ***2Z***. Thus, by introducing a shorter olefinic carboxyl side chain, we reduced the total number of rotatable bonds from seven (**1**) to five (**2*Z***). An even more rigid, cyclized analogue **21*E*** was prepared by condensation of 4-chlorobenzaldehyde **2d** with 1-indanone, reduction of the resulting cyclized chalcone, HWE reaction, and subsequent ester hydrolysis (Scheme 1). 21***E*** was isolated as enantiomeric mixture exclusively in the (*E*)-form.

In another subset of compounds, we replaced the ring **A** benzylic methylene by oxygen or sulfur. The strategy for the synthesis of these heteroanalogues of **2*Z*** is illustrated in Scheme 2. Bromoacetophenone was subjected to an S_N reaction with 4-chlorophenol (**14c**) and 4-chlorophenyl mercaptane **15c**, respectively, to yield 2-(4-chlorophenoxy)acetophenone (**14b**) and 2-(4-chlorophenylthio)acetophenone (**15b**). The final compounds, (*E*)- and (*Z*)-4-(4-chlorophenoxy)-(**14*E***,**14*Z***) and (*E*)-4-(4-chlorophenylthio)-3-phenylbut-2-enoic acid (**15*E***), were obtained via HWE reaction (method C) and hydrolysis (method D) analogously to the 3,5-diphenylpentenoic acids.

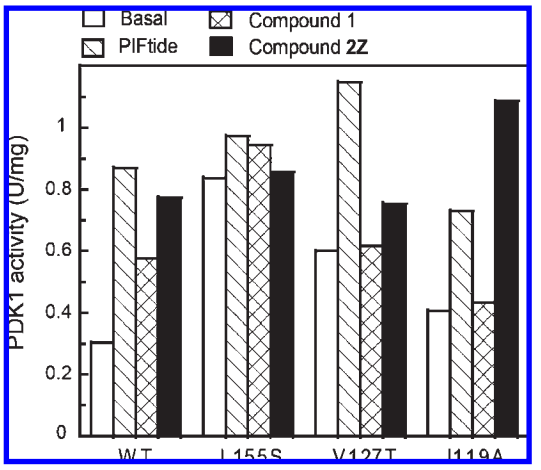

Figure 2. Biochemical evidence from site-directed mutagenesis that the PIF-binding pocket of PDK1 is the target site of **2*Z***. The effect of **2*Z*** on PDK1 specific activity was measured with recombinant wild type enzyme and PIF pocket-binding mutants as indicated. Mutation of valine-127 to threonine abrogates the activation of PDK1 by **2*Z*** but not by the 22 amino acid residue peptide PIFtide. For comparison, results obtained with the original compound 1 are also given. Concentrations of the compounds used were 2 μM for PIFtide and 20 μM for **1** and **2*Z***.

In addition, we prepared heterocyclic analogues via two different synthetic pathways (Scheme 3). Rap−Stoermer reaction of salicylaldehydes **16c** and **17c** with phenacyl bromide (method E) provided the substituted 2-benzoylbenzofurans **16b** and **17b**,[27] while synthesis of 2-(4-chlorobenzoyl)benzothiophene (**18b**) was accomplished by a one-step nucleophilic aromatic displacement of an activated nitro function by mercaptoacetophenone followed by an intramolecular aldol condensation.[28] The heterocyclic precursors were further processed to the corresponding acrylic acids (**16**−**17**, **18*E***, **18*Z***) analogously to compounds **2b**−**13b**. Finally, we also reduced the acrylic acids (**16*E*/*Z*a**−**17*E*/*Z*a**) to the corresponding propionic acids (**19a**−**20a**) by means of a catalytic transfer hydrogenation (method F) using sodium hypophosphite in combination with Pd/C.

2. Biological Activity. 2.1. Biochemical Evidence that Compound 2Z Activates PDK1 by Binding to the PIF-Binding Pocket. To measure the effect of compound **2*Z*** on the PDK1 catalytic activity, we performed a radioactive kinase activity assay employing T308tide, a peptide derived from the activation loop of PKB, as a substrate. Similarly to the 24 amino acid polypeptide PIFtide, characterized to bind to the PIF-binding pocket and activate PDK1,[4] compound **2*Z*** increased the activity of wild type (wt) PDK1 with the same activation efficacy (data for PIFtide not shown) (Figure 2). In addition, **2*Z*** displayed a 4-fold lower AC_{50} than the hit compound **1** (Table 1).[22] To biochemically characterize the binding site of **2*Z*** on PDK1, we compared the ability of **2*Z*** to activate wt PDK1 vs PDK1 proteins mutated within the PIF-binding pocket. The mutant $PDK1^{L155S}$, in which the character of the PIF-binding pocket is completely changed, could not be activated by PIFtide nor by **2*Z***, suggesting that the PIF-binding pocket site was required by both effectors. In contrast, the ability of **2*Z*** to activate PDK1 was lost toward the $PDK1^{V127T}$ mutant while this mutant was still activated by PIFtide. This was not surprising because previous work had shown that when V127 was mutated to a larger hydrophobic residue (Leu), the mutant PDK1 protein also retained

Scheme 3. Synthesis of Compounds **16**−**17**, **18*E***, and **18*Z***[a]

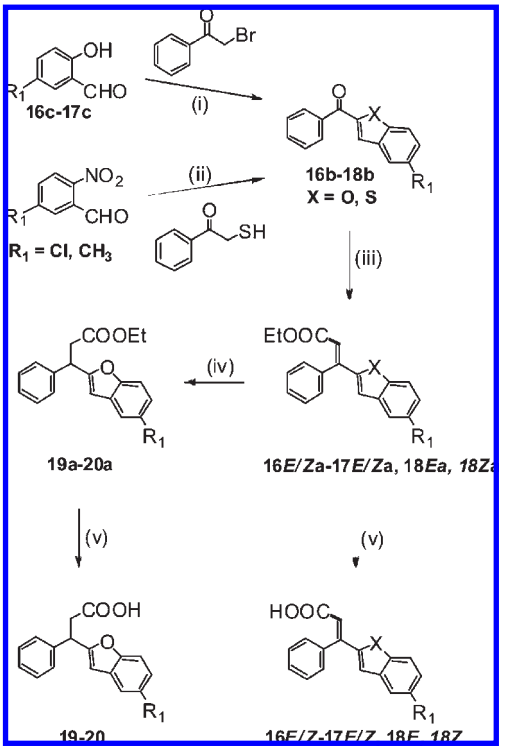

[a]Reagents and conditions: (i) method E: K_2CO_3, DMF, reflux, 2 h; (ii) K_2CO_3, DMF, 0 °C to rt, 3 h; (iii) method C: triethyl phosphonoacetate, NaH, DME, 80 °C, 4 h; (iv) method F: $NaH_2PO_2 \cdot H_2O$, 10% Pd/C, $EtOH/H_2O$, 60 °C, 2.5 h; (v) method D: NaOH, EtOH, rt, 3 h.

the ability to bind and be activated by PIFtide, and to efficiently interact and phosphorylate SGK, a substrate that relies on the binding of its hydrophobic motif to the PIF-binding pocket on PDK1.[22] Thus, it appears that HM polypeptides do not rely so heavily on the identity of the residue at position 127, while the much smaller compound **2*Z*** required a valine residue at position 127 within the hydrophobic PIF-binding pocket. Interestingly, the $PDK1^{I119A}$ mutant was well activated by **2*Z***, whereas the activatory potencies of both compound **1** and PIFtide were affected by this mutation. Altogether, the mutagenesis results suggested that the binding of **2*Z*** was indeed within the hydrophobic PIF-binding pocket. However, there were significant differences on the requirements between **2*Z***, **1**, and PIFtide, which had also been suggested to bind to the same site.

The cocrystallization of **2*Z*** with PDK1 confirmed that binding occurs exclusively in the PIF-binding pocket (Figure 3; crystallographic details together with studies on the allosteric mechanism of PDK1 activation by low molecular weight compounds will be published elsewhere[25]). The complex structure showed that the two phenyl rings bound to the two hydrophobic subpockets separated by L155 and bordered by V127, explaining the lack of activity of compound **2*Z*** on PDK1 proteins mutated at these sites (Figure 2). In contrast, the ethyl branch of I119 borders one side of the pocket and interacts only marginally with the chlorine of **2*Z***, therefore explaining why the substitution for a smaller hydrophobic residue did not affect the ability of **2*Z*** to activate PDK1. Altogether, the crystal structure of the catalytic domain of PDK1 was in agreement with the biochemical studies performed here in solution with PIF-binding pocket mutants

Table 1. Effect of Compounds on Catalytic Activity of PDK1 and Thermodynamic Characterization of Binding

			Kinase activity assay		ITC					
No.	**Structure**		A_{max} [a] fold	AC_{50} [a,b] μM	K_a [c] M^{-1}	K_d [c] μM	ΔH [d] kcal/mol	$T\Delta S$ [e] kcal/mol	ΔG [f] kcal/mol	ΔH/ΔG %
	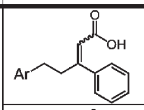									
	Ar									
2*Z*	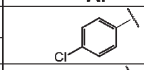		4.0 [g]	8.0 [g]	9.67E4	10.3	-1.82	4.87	-6.73	27.1
2*E*			n.e.	n.e.	-	n.b.				
3*Z*	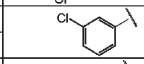		2.2	9.5	-	n.d.				
3*E*			n.e.	n.e.	-	n.d.				
4*Z*	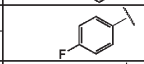		3.3	41.0	-	n.d.				
4*E*			n.e.	n.e.	-	n.d.				
5*Z*	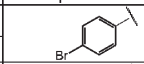		3.9	9.8	4.78E4	20.9	-3.07	3.20	-6.32	48.6
5*E*			n.e.	n.e.	-	n.d.				
6*Z*	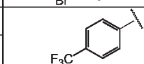		4.4	7.1	9.66E4	10.4	-1.94	4.79	-6.73	28.8
6*E*			n.e.	n.e.	-	n.d.				
7*Z*	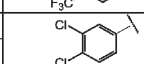		2.4	2.8	7.18E4	13.9	-3.71	2.80	-6.56	56.6
7*E*			n.e.	n.e.	-	n.d.				
8*Z*	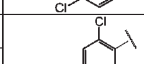		2.1	4.7	1.71E5	5.9	-2.08	4.93	-7.07	29.5
8*E*			n.e.	n.e.	-	n.d.				
9*Z*	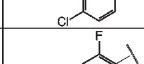		3.9	4.0	1.62E5	6.2	-1.79	5.19	-7.15	25.0
9*E*			n.e.	n.e.	-	n.b.				
10*Z*	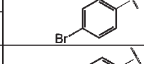		1.4	>30	-	n.d.				
10*E*			n.e.	n.e.	-	n.d.				
11*Z*	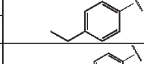		3.2	6.0	-	n.d.				
11*E*			n.e.	n.e.	-	n.d.				
12*Z*	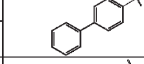		3.5	6.0	7.26E4	13.8	-4.56	1.96	-6.67	68.3
12*E*			n.e.	n.e.	-	n.b.				
13*Z*	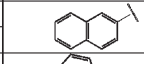		3.1	7.6	9.63E4	10	-4.09	2.60	-6.73	60.8
13*E*			2.2	8.8	-	n.b.				
	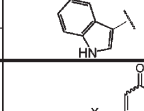									
	X									
14*E*	O		3.0	22.8	-	n.d.				
14*Z*	O		n.e.	n.e.	-	n.d.				
15*E*	S		2.6	22.8	-	n.d.				
	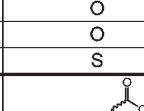									
	R	**X**								
16 [h]	Cl	O	3.2	31.6	-	n.d.				
17 [h]	Me	O	3.1	41.3	-	n.d.				
18*E*	Cl	S	3.1	13.2	-	n.d.				
18*Z*	Cl	S	n.e.	n.e.	-	n.d.				
	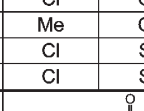									
	R									
19	Cl		2.9	19.0	-	n.d.				
20	Me		2.7	29.1	-	n.d.				
21	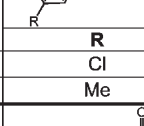		1.8	30	-	n.d.				

[a] Mean value of at least two independent experiments, standard deviation < 20%. [b] As a particularity for compounds with activatory properties, it was necessary to indicate the maximum activation that was achievable with a compound, as compared to the basal activity of PDK1 (set to 100%). Error bars were calculated based on two independent titrations of PDK1 with **12Z** as follows: [c] Standard deviations for K_a and K_d are of 11%. [d] Error bar for $\Delta H = +0.30$ kcal/mol. [e] Error bar for $T\Delta S = +0.37$ kcal/mol. [f] Error bar for $\Delta G = +0.07$ kcal/mol. [g] Values were taken from ref 25. [h] Mixture of isomers, ca. 75% *Z*/25% *E* for **16**, and 70% *Z*/30% *E* for **17**. n.e.: no effect; n.b.: no binding; n.d.: not determined.

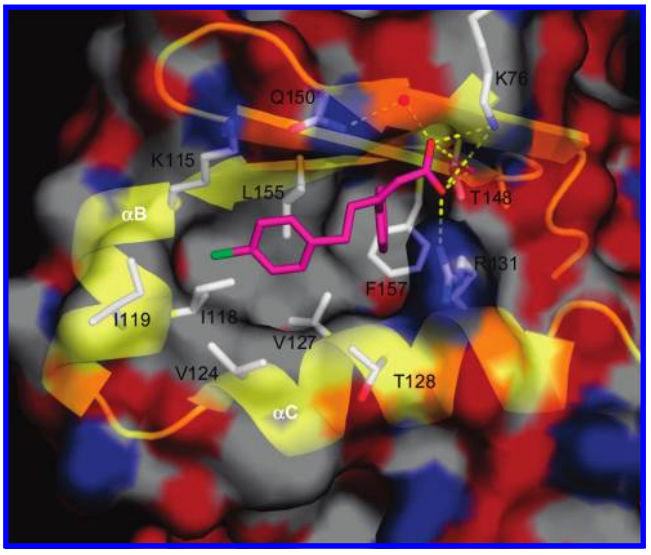

Figure 3. Compound **2*Z*** bound in the PIF-binding pocket of PDK1. The pocket is bordered by the αC helix and the short αB helix as indicated. Dashed yellow lines display the interactions of the carboxylate group with R131, T148, and K76 and with Q150 via a water molecule (red ball). L155 divides the hydrophobic groove into two subpockets that are occupied by the benzene rings. Phenyl ring B (3-phenyl, see Figure 1) additionally contributes to the binding energy by forming edge-to-face CH−π interactions with F157. As shown in Figure 2, mutation of V127 to threonine abolished the activation by **2*Z***. The structure was generated using PyMOL (http://pymol.sourceforge.net/).

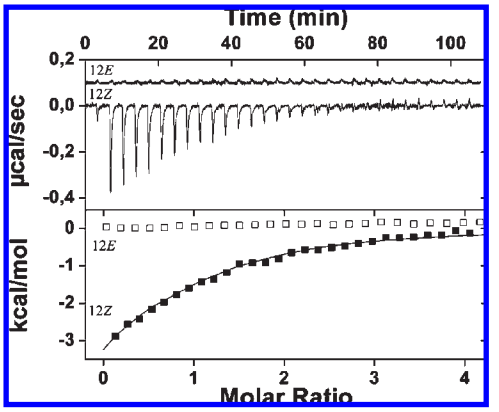

Figure 4. Characterization of **2*Z*** and **2*E*** isomers interactions with $PDK1_{50-359}$ by ITC. The top panel shows the raw heat signal for successive injections of dissolved compounds **12*Z*** and **12*E*** into a $PDK1_{50-359}$ solution at 20 °C. The bottom panel shows the integrated heats of injections corrected for heats of dilution for **12*Z*** (filled squares) and **12*E*** (open squares), with solid lines corresponding to the best fit of the data to a bimolecular binding model. No binding of compound **12*E*** to $PDK1_{50-359}$ is detected in conditions where **12*Z*** shows clear binding. Thermodynamic parameter values are given in Table 1.

of full length PDK1, further confirming the PIF-binding pocket as the binding site for **2*Z***.

2.2. Dependency of Allosteric Potency and Binding of the Compounds on Electrostatic Interactions Involving the Carboxyl Group. The **2*Z***/PDK1 cocrystal structure had revealed that the carboxylate of **2*Z*** interacted with the receptor site in a network of ionic and H-bonds, comprising interactions with K76 (ε-NH_2), T148 (OH), R131, and water-mediated with the amide of Q150 (Figure 3).[25] Thus the carboxylate mimicked the phosphate group of phosphoserine/threonine residues from natural ligands, which is expected to bind to the equivalent site. In good agreement with this cocrystal structure result, we found that the potency to activate PDK1 was associated only with the geometric isomers carrying the carboxy group cis relative to the phenyl ring **B** (generally termed "cis isomers" for easier readability in the following = *Z* isomer for **2*Z***/**2*E***−**12*Z***/***E***, *E* isomer for **14*E***/**14*Z*** and **18*E***/**18*Z***), whereas the isomers with the opposite configuration (termed "trans isomers" in the following) were mostly inactive (Table 1). The only exception was **13*E***, which displayed only a slight increase of the AC_{50} compared with the *Z* form but, however, was activating with only low efficacy (2.2 fold, Table 1).

If the ring systems of the trans isomers would bind to the PIF-binding pocket similar to the two phenyls from **2*Z***, the respective carboxy group would point to the opposite direction (see Figure 3). Therefore, on the basis of the crystal structure of PDK1 bound to **2*Z***, it becomes clear that the carboxy moiety of the trans isomers cannot interact with the same type and quantity of bonding as seen with the cis isomer ***2Z***. The trans orientated carboxy group could potentially form H-bonds directly with Q150; however, the lack of activity of the respective trans isomers **2*E***, **9*E***, **12*E***, **14*Z***, and **18*Z*** indicated that a broader range of interactions with phosphate binding site residues were required for prompting the activation of PDK1. Furthermore, the complete lack of activity of the **2*Z*** ethyl ester derivative (*Z*)**-2a** also corroborated that in particular the strong ionic interactions with phosphate binding site residues neighboring the hydrophobic PIF-binding pocket provided an important contribution to the ability to activate PDK1 (data not shown).

The above data indicated that all the cis isomers **2*Z***−**12*Z***, **14*E***, and **18*E*** activated PDK1, whereas activation potency of the corresponding trans isomers was completely absent or strongly reduced in the case of **13*E***. Next we performed calorimetry experiments to investigate whether the trans isomers show a complete lack of binding or if there is binding that is uncoupled from allosteric activation. We found that under identical experimental conditions, all the trans isomers analyzed, **2*E***, **9*E***, **12*E***, and **13*E***, did not interact with PDK1 (estimated detection limit: $K_d > 100\ \mu M$) (Table 1), in contrast to the corresponding cis isomers, which all bound in a 1:1 stoichiometry. For a direct comparison, example calorimetric data are shown for the stereoisomers **12*Z*** and **12*E*** in Figure 4.

On the basis of the current data, we cannot explain why **13*E*** still displayed a weak activation of PDK1 while there was no detectable binding in the ITC experiments. Because the ITC measurements were performed in the absence of ATP, it could be speculated that in the activity assays, allosteric cooperative effects triggered by ATP binding might enable interaction of **13*E*** with the PIF-binding pocket, thus stabilizing a slightly more active conformation of PDK1; thereby the indole ring might promote the binding by H-bond interaction with Q150, thus distinguishing **13*E*** from the other trans configured compounds that were analyzed by ITC.

In general, our ITC findings confirmed that strong binding was only possible when the carboxy group was in the cis configuration. Furthermore, the similar results obtained with the different compound analogues suggested that all cis compounds may be docked to the phosphate binding site in a similar way, further positioning the phenyl ring **B** into

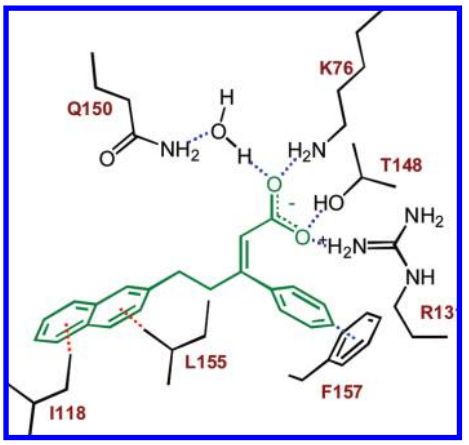

Figure 5. Scheme summarizing the specific interactions of lead compound **12*Z*** with the PDK1 PIF-binding pocket. Blue dotted lines denote interactions that have been identified for the analogue **2*Z*** in the co-crystal structure with PDK1; red dotted lines indicate the assumed interactions as inferred from the ITC experimental data.

the same subpocket on the PDK1 PIF-binding pocket as experimentally described for **2*Z***.

2.3. Interrelationships between Structure, Activity, and Thermodynamic Binding Signature. We found that phenyl ring B from **2*Z*** (as defined in Figure 1) participated in an edge-to-face CH$-\pi$ interaction with F157 (Figure 3). Such T-shaped interactions between benzene dimers are stabilized by 2.4 kcal/mol in the gas phase[29] and were found to be the most favored formation in solution.[30] The distance between the two phenyl components of the T-shape interaction (3.22 Å between the **2*Z*** C4 and the ring center of F157 in the cocrystal) is significantly shorter than the sum of the C$-$H$\cdots$C van der Waals radii and thus indicative of a rather strong interaction. Therefore, to investigate the effect of different ring substitutions on the potency of the compounds, we did not modify ring **B** but rather focused on substitutions on ring **A**. Indeed, our working model of the compound **2*Z*** binding suggested larger unfilled space in the ring A subpocket binding site (cf. Figure 3).

To optimize ring **A**, the halogen substituents were systematically varied in type and position. We observed no major differences in activation potency (AC_{50}) among the compounds carrying *p*-Cl, *p*-Br, or *p*-CF_3 substituents (**2*Z***, **5*Z***, **6*Z***, Table 1), whereas fluorine in **4*Z*** was not tolerated and caused a large increase in AC_{50}. The highest activation efficacy (A_{max}) of the compound series was achieved by the *p*-CF_3 substituent. Shifting the *p*-Cl to the *m*-position (**3*Z***) adversely affected the potency to activate (2.2 fold) because it remained also low in the 3,4-dichloro substituted compound **7*Z***.

Both dichloro substituted compounds, **7*Z*** and **8*Z***, showed remarkable properties that were distinct among each other and from the monosubstituted compounds. This indicated that it was possible to control the binding and allosteric properties of PIF-binding pocket directed compounds by selecting different substitution positions. The 3,4-dichloro substitution (**7*Z***) was breaking the general correlation between AC_{50} and K_d as discussed below (Figure 6B). Our thermodynamic data indicated that part of the binding entropy seen with **2*Z*** was lost, suggesting that the 3-Cl was impeding the hydrophobic interaction of the substituted phenyl ring with the pocket, although a precise explanation was lacking.

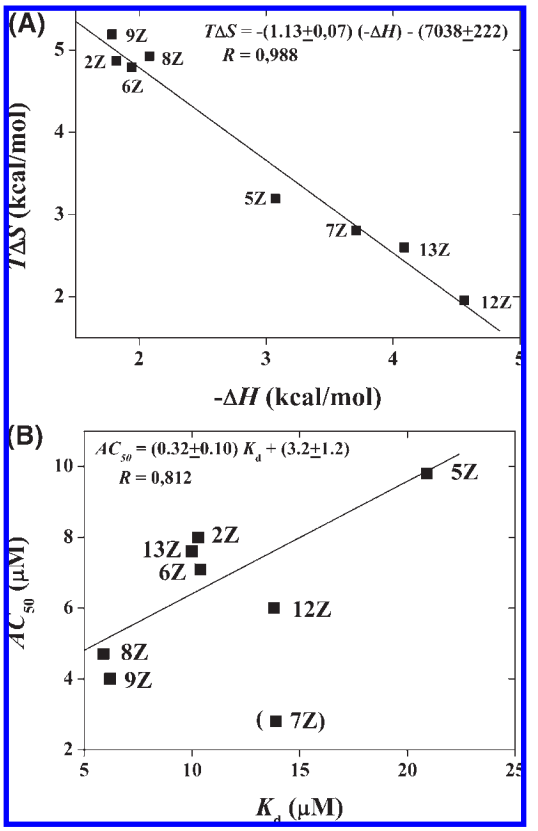

Figure 6. General correlations based on calorimetric measurements. (A) Enthalpy$-$entropy compensation phenomenon observed upon binding of *Z* isomers to PDK1. Large changes in the binding enthalpies (ΔH) and binding entropies ($T\Delta S$) were measured. However, the observed linear relationship between the ΔH and $T\Delta S$ values with a slope of 1 shows that a favorable increase in binding enthalpy was compensated by an equal unfavorable loss of entropy in the binding free energy ($\Delta G = \Delta H - T\Delta S$), which left nearly unchanged the binding affinity ($K_d = \exp[\Delta G/RT]$). (B) A gross linear correlation was observed between the AC_{50} values for PDK1 activation and the dissociation constants as measured by ITC. This correlation suggested that, for most compounds, the binding affinity to the intermediate active conformation of the kinase, which might be represented rather by the AC_{50}, does not differ strongly from the affinity to the activated conformation of the kinase, which might be described by the K_d. Only for compound **7*Z*** (not used to calculate the trend line), a low AC_{50} was associated with an overproportionally high K_d.

The 2,4-dichloro substitution pattern in **8*Z***, however, had a very distinct and interesting effect on the allosteric potency, as the *o*-chlorine induced a rather "antagonist" like behavior of the compound: although **8*Z*** displayed one of the lowest AC_{50} values and even the lowest K_d, the potency to allosterically activate PDK1 decreased to about half of the A_{max} of **2*Z***. In contrast to the 3,4-dichloro substituted analogue **7*Z***, **8*Z*** displayed a predominantly entropy-driven binding (Table 1). Thus, although we cannot provide a final answer based on our current data, the more entropy-driven binding of ring **A** in **8*Z*** might allow a greater flexibility of positioning within the hydrophobic pocket in order to avoid a steric clash of the 2-chlorine with either T128 or Q150 (compare with ring **A** position of **2*Z***, Figure 3), whereas the binding positions might be more restricted in the case of highly directed H-bonds and dispersion forces that usually contribute to the enthalpy term.

Such an entropy-enabled binding shift might propagate into suboptimal interaction of the 8Z carboxyl side chain with R131, resulting in a reduced allosteric activation without compromising binding affinity. A comparison of **8*Z*** with **9*Z*** showed that entropy-driven binding alone was not sufficient to confer "antagonist"-like properties, rather a steric impact, like from the *o*-chlorine, was also required. This was corroborated by the fact that the maximum activation potency of the 4-bromo derivative **5*Z*** was not affected when a smaller *o*-fluorine was introduced (cf. **9*Z***) despite the significant increase in the entropy/enthalpy ratio of binding. It will be interesting to see whether **8*Z*** binds to and stabilizes the intermediate active, basal conformation of the PIF pocket without causing major conformational changes.

Because the 3,4-dichloro substitution (**7*Z***) decreased the AC_{50} almost 3-fold compared to the 4-chloro compound **2*Z***, we wanted to explore further enlargement of the ring system at 3,4-positions, leading to the synthesis of **12*Z*** and **13*Z***. In contrast to **7*Z***, the ring extension by a second phenyl in **12*Z*** did not abolish the activation potency. Again, the application of isothermal calorimetry allowed us to gain insight in the quality of interactions between the bicyclic rings of **12*Z***/**13*Z*** and the PIF binding pocket. Both compounds showed the highest $\Delta H/\Delta G$ ratios in the analyzed series (**12*Z***: 68.3%, **13*Z***: 60.8%) due to a marked increase of the enthalpy relative the entropy of binding (Table 1). This was in sharp contrast to all halogen-substituted phenyl analogues (with the exception of **7*Z***). Considering that the unsubstituted bicyclic rings have a higher π−electron density combined with a larger surface, the increase of the binding enthalpy argued for a stronger contribution of CH−π interactions than present with the halogen-substituted phenyl rings. Although the enthalpy for one unit CH−π interaction is small, around 1 kcal/mol,[31] we hypothesized that multiple CH groups participated simultaneously in interactions with π electrons, thus adding up to a significant increase in enthalpy, consistent with our experimental data. According to the cocrystal structure, the following residues of the PIF-binding pocket were possible candidates for a putative interaction with the extended π−electron system of **12*Z*** or **13*Z***: most certainly the geminal dimethyl of L155, and, depending on which rotamer of the naphthyl or indolyl linking bond is preferred, either the terminal methyl of I118 or γ-methylene of the K115 side chain (cf. Figure 3). Both of the latter residues are within reach of the bicyclic rings of **12*Z*** and **13*Z***, and the two possible corresponding rotamers could dock into the subpocket provided that the available space is slightly increased by a movement of the I119 chain. Because terminal methyls of Leu, Ile, or Val are more commonly found in CH−π interactions,[31] we included a hypothetical interaction between the naphthyl of **12*Z*** and the methyl of I118 in the interaction scheme for **12*Z*** (Figure 5).

It is conceivable that the enthalpy gain due to the assumed reinforcement of CH−π interactions could compensate for a less favorable entropy associated with potential movements of side chains. This hypothesis was supported by the differential activation potencies of **10*Z*** and **11*Z***; both compounds can only bind to the PIF-subpocket in the same way as the chlorophenyl ring of **2*Z*** when I119 moves away in order to avoid a steric clash (cf. Figure 3). While the active compound **11*Z*** offers potential for additional CH−π interactions, which could compensate for an entropic penalty, the *p*-ethyl substituted **10*Z***, which is incapable of forming additional CH−π bonds, was nearly inactive.

For the phenyloxy- and phenylthio-substituted series, both a slight reduction of the maximum activation of PDK1 and an increase of the AC_{50} values was noted compared with **2*Z*** (**14*E*** and **15*E***). The *trans*-4-chloro-phenoxy compound **14*Z*** was completely inactive. This suggested that the compounds bound to the PDK1 PIF-binding pocket in a similar way but interacted with the key allosteric residues in a slightly different manner so that full activation of the catalytic activity could not occur. In addition, we concluded that the oxygen of **14*E*** was probably too distanced from the Q150 amide or from the T128 hydroxyl for H-bond interactions (cf. Figure 3). Rather, the increase in polarity adversely affected hydrophobic interactions with the pocket.

Next, the rather flexible structure of **2*Z*** and its derivatives was rigidified in order to increase binding affinity but also to probe the potential overall conformation required for a compound to bind to the PIF-binding pocket. Our initial working model suggested that a benzoannelated heterocycle linking carbon 4 with the ortho position of ring **A** in **2*Z*** might be compatible with the presumed V-shaped binding mode of an active compound. In fact, the conformationally constraint versions of **14*E*** and **15*E*** could significantly activate purified PDK1 (compounds **16**, **17**, and **18*E***), providing clues on the conformation required for a HM/PIF-binding pocket directed compound to trigger activation. With the benzofuran compounds **16** and **17**, chromatographic separation of the *E* and *Z* isomers was not possible, thus precluding separate determination of the biological activity. However, from the benzothiophene compounds, the *E* isomer was a considerably better activator of PDK1 then the *Z* form, thus suggesting that cyclized and open chain analogues have similar binding modes in the PIF-binding pocket. Moreover, this result suggests that the pure *E* isomer from **16** would have a lower AC_{50} in the same range as **18*E*** because the *Z* isomer in the mixture very probably did not contribute to the activity. In summary, cyclizations involving ring **A** did not increase potency, probably because they abolished part of the flexibility required to optimally adapt to the pocket shape. Nevertheless, the remaining activity of **16** and **18*E*** proved that a broad range of angles is tolerated for docking of the ring system equivalent to ring **A** (Figure 1) to the subpocket. The narrow subpocket for the unsubstituted phenyl ring (ring **B**) forces a steeper docking, thus the 120° angled benzothiophene in **18*E*** must bind in a considerably more flat position in the other subpocket than ring **A** from **2*Z***, where the prolonged axes of the phenyl rings enclose an angle of approximately 46° (measured in the cocrystal structure).

An analogous cyclization involving ring **B** led to **21** with a strongly reduced maximum activation of PDK1 as compared to **2*Z***. This result indicated another essential property for PDK1 activator compounds, which is the ability of ring **B** to rotate out of the double bond plane. In accordance with this experimental finding, the corresponding dihedral angle in the cocrystal conformation of **2*Z*** was 118°.

2.4. Overall Correlations between Enthalpy and Entropy of Binding and the Biological Activity Parameters of Allosteric PDK1 Activators. Regardless of the pivotal ionic interaction which contributed essentially to the binding of all active compounds, we found a surprisingly broad thermodynamic binding spectrum from mainly entropy-driven to predominantly enthalpy-driven binding. A correlation analysis

involving the thermodynamic binding signature and the activity data revealed two strong relationships; as the most obvious correlation, we identified a sharp enthalpy−entropy compensation effect, which has been described for many ligand−receptor systems such as agonists and antagonists interacting with membrane receptors[32−34] and inhibitors binding to HIV protease[35] (see $\Delta H/T\Delta S$ correlation, Figure 6A). This effect describes the fact that among a series of compound analogues with comparable size, any increase in binding enthalpy is accompanied by a loss of entropy to about the same degree, leading to little or no change in the binding affinity.[36,37] The compensation effect was most obvious when comparing the group of halogenated compounds (**2*Z***, **6*Z***, **8*Z***, and **9*Z***) with **12*Z*** and **13*Z*** (Figure 6A). The bicyclic aromatic rings caused binding with highly favorable enthalpy, probably due to additional CH−π interactions as described above (Figure 5). Our ITC data indicated that the additional binding enthalpy was gained at the cost of entropy, accounting for the enthalpy−entropy compensation in the concrete case. A possible explanation for the concomitant loss of entropy with **12*Z*** and **13*Z*** could be that due to the higher polarity of the π−electron-rich rings, the contacting water molecules are less ordered and less entropy is gained upon water release from the compound. In contrast, fewer enthalpically favorable van der Waals or CH−π interactions are possible with one phenyl ring where the density of the π−electrons is further decreased by halogen substituents. Apparently, this loss of H-bond capacity in the halogenated compounds was exactly balanced out by an opposite increase in hydrophobic interaction, giving raise to the entropy term. These mutual compensation processes prevented significant changes in the total binding free energies of compounds (compare e.g. **2*Z***, $\Delta G = -6.73$ kcal/mol with **12*Z***, $\Delta G = -6.67$ kcal/mol), which otherwise differed substantially in their $\Delta H/\Delta G$ ratio (Table 1). This phenomenon is not uncommon in the lead optimization process and has to be overcome in order to increase binding affinity. (see Section 2.5 below).

Another relationship became apparent when the thermodynamic binding profiles were correlated with the activatory potency of the compounds. We observed a rough correlation between the AC_{50} values for PDK1 activation and the dissociation constants as measured by ITC (Figure 6B). This correlation suggested that for most compounds, the binding affinity to the intermediate active conformation of the kinase, which might be represented rather by the AC_{50}, does not differ strongly from the affinity to the activated conformation of the kinase, which might be described by the K_d. The variations in activation efficacy (A_{max}) did not affect this correlation. The relationship between AC_{50} and K_d was not self-evident because binding to the intermediate active state and dissociation of the complex after the conformational change could be perceived as two separate events characterized by divergent affinity constants. Our finding rather suggests that during the allosteric activation by the majority of compounds, only subtle and rapid changes occur within the PIF-binding pocket itself, while the overall geometry of the PIF-binding pocket remains unaltered.

2.5. Implications of the Calorimetric Characterization for Lead Selection and Optimization. In a scenario where the goal is to increase binding affinity of small molecules, a proven strategy is to choose as lead candidates compounds that show enthalpy-dominated binding.[35,38] The reason is that enthalpy-driven interactions are more difficult to engineer because they arise primarily from specific van der Waals and H-bonding interactions, for which a good geometric complementarity between the involved functional groups of drug and receptor is a prerequisite. To optimize the entropy contribution on the other hand has proven much easier, as this is almost inevitably achieved by introducing nonpolar groups that increase the hydrophobic effect.[39] From the perspective of allosteric modulators, it might be worth discussing whether **8*Z***, which displayed stronger binding in connection with the opposite trend in activation potency, should not be pursued in parallel as lead compounds toward the development of nonactivators or even allosteric inhibitors. However, because very high affinity can only be achieved if both enthalpy and entropy contribute favorably and in a balanced manner to the binding free energy,[38,40] enthalpy-dominated binders are doubtlessly the preferred starting point for lead optimization. Moreover, it was reported by Nezami et al. that in order to overcome the enthalpy−entropy compensation effect, an optimal balance with the free energy partitioned approximately as one-third enthalpy and two-thirds entropy ($T\Delta S$) was required.[40] Only compounds with this combination reached nanomolar affinity to the target plasmepsin II in the reported case; the same conclusion could also be drawn for allosteric glycogen phosporylase inhibitors in a recent study.[38] In that sense, calorimetric analysis has disclosed **8*Z*** rather as a "dead end" because the balance has been reached already ($\Delta H/\Delta G = 29.5\%$) and any addition of another chemical moiety would provoque enthalpy/entropy compensation effects without substantially increasing ΔG. Similarly, the thermodynamic binding data for **9*Z*** revealed the compound as a less appropriate starting point to escape enthalpy−entropy compensation, even though the AC_{50} was two times lower than that of **2*Z*** (Table 1).

In summary, **12*Z*** and **13*Z*** were found to possess the most ideal thermodynamic lead profile among the compounds analyzed by ITC because the enthalpic term strongly predominates the binding free energy.

4. Conclusions

The compounds presented herein represent a rare case of truly allosteric compounds targeting a regulatory binding site on a protein kinase catalytic domain that is not adjacent to or overlapping with the ATP binding site. It should be mentioned that many inhibitors reported in the literature to be "allosteric" still bind to the ATP binding site at least partially. As in the case of imatinib mesylate (gleevec), the term is used to signify that an inactive, open conformation of the kinase is stabilized.[21] This study is, to the best of our knowledge, the first one correlating the structural motifs of allosteric activators with both the effects on catalytic activity (A_{max} and AC_{50}) and the energetics of the interaction (quantified by isothermal titration calorimetry).

Altogether, our work might pave the way to the development of allosteric modulators for PDK1 based on the following findings: (i) We have defined the minimum requirements for a small compound to function as a PDK1 activator, two aromatic moieties connected by an aliphatic chain, bearing a two atom membered side chain with a free carboxylic group; a V-shaped overall conformation of the aryl rings toward each other is also required to achieve complementarity to the binding pocket.

These prototype compounds, despite the low molecular masses, already displayed activities in the low μM range, suggesting that mass and ligand efficiency should remain in a reasonable range after lead optimization. (ii) Some important CH$-\pi$ interactions between ligand and receptor that can essentially contribute to increased selectivity and potency of PIF-pocket directed compounds have been identified by virtue of their favorable binding enthalpy. (iii) Calorimetric analysis revealed compounds binding with variable proportions of entropy and enthalpy, allowing for selection of appropriate structures as starting points to further improve potency. Thus we were able to establish that the HM/PIF-binding pocket of PDK1 as a druggable site despite being located at the protein surface and physiologically participating in extended protein−peptide interactions.

Because hydrophobic pockets homologous to our target binding site are conserved in many protein kinases comprising the whole AGC family, our approach may be suitable for similar developments of allosteric modulators for a broad range of kinase targets. Thereby the mechanisms of action would consist of allosteric effects on the kinase catalytic activity, blocking of inter- or intramolecular protein−protein interactions, or a combination of both, allowing a more subtle manipulation of intracellular signaling pathways.

In contrast to the more established kinase inhibition strategies, direct allosteric activation of a protein kinase is a rather new scientific concept. In the case of PDK1, activation of the catalytic activity is achieved by binding to the HM/PIF-binding pocket, which at the same time blocks the activation of all substrates that require transient interaction with the pocket. This is the case for all known PDK1 substrates, including S6K, RSK, and some PKC isoforms but not for PKB. Thus the compounds might act differentially on the two subsets of PDK1 substrates, which either require docking interaction with the PIF-binding pocket or not. Hence, in-depth investigation of the compounds' effects on the cellular signaling pathways, using genetic tools and detailed phosphorylation analysis, are required and will be subject of our future studies. In particular, detailed analyses in a cellular setting will be required to study the biological effects of PIF-binding pocket targeting compounds with high (e.g., **6*Z***) vs low (e.g., **8*Z***) concomitant allosteric activation of PDK1 catalytic activity.

5. Experimental Section

5.1. Chemistry. 5.1.1. General. Solvents and reagents were obtained from commercial suppliers and were used without further purification. Flash column chromatography was carried out using silica-gel 40 (35/40−63/70 μM) with hexane/ethyl acetate mixtures as eluents, and the reaction progress was determined by TLC analysis on Alugram SIL G/UV$_{254}$ (Macherey-Nagel). Visualization was accomplished with UV light and $KMnO_4$ solution. ^{1}H NMR, ^{13}C, and 2D-NOESY spectra were recorded at 500 MHz using a Bruker DRX-500 spectrometer. ^{1}H shifts are referenced to the residual protonated solvent signal (δ 2.50 for DMSO-d_6 and δ 7.26 for $CDCl_3$) and ^{13}C shifts are referenced to the deuterated solvent signal (δ 39.5 for DMSO-d_6 and δ 77.2 for $CDCl_3$). Chemical shifts are given in parts per million (ppm), and all coupling constants (J) are given in Hz. The purities of the tested compounds **2*Z*-21** were determined by HPLC coupled with mass spectrometry and were higher than 95% for all compounds except **8*E*** and **13*Z***, which exhibited at least 93% and 94% purity, respectively. Mass spectrometric analysis (HPLC-ESI-MS) was performed on a TSQ quantum (Thermo Electron Corporation) instrument equipped with an ESI source and a triple quadrupole mass detector (Thermo Finnigan, San Jose, CA). The MS detection was carried out at a spray voltage of 4.2 kV, a nitrogen sheath gas pressure of 4.0×10^5 Pa, an auxiliary gas pressure of 1.0×10^5 Pa, a capillary temperature of 400 °C, capillary voltage of 35 V, and source CID of 10 V. All samples were injected by autosampler (Surveyor, Thermo Finnigan) with an injection volume of 10 μL. A RP C18 NUCLEODUR 100−3 (125 mm × 3 mm) column (Macherey-Nagel) was used as stationary phase. The solvent system consisted of water containing 0.1% TFA (A) and 0.1% TFA in acetonitrile (B). HPLC-method: flow rate 400 μL/min. The percentage of B started at an initial of 5%, was increased up to 100% during 16 min, kept at 100% for 2 min, and flushed back to the 5% in 2 min. All masses were reported as those of the protonated parent ions. Melting points were determined on a Mettler FP1 melting point apparatus and are uncorrected.

5.1.2. Method D: Hydrolysis. A solution of the corresponding ester (**2−13*E*/*Z*a**) (1 equiv) and $NaOH_{aq}$ (3 equiv) in EtOH was refluxed for 4 h. After the completion of reaction, the cooled mixture was poured into water (30 mL), acidified to pH 2 with 10% HCl, and extracted with ethyl acetate (3 × 20 mL). The organic layers were collected, washed with brine (20 mL), dried over $MgSO_4$, and evaporated to afford a residue, which was purified by crystallization to afford the acids.

5.1.2.1. (*E*)-5-(4-Chlorophenyl)-3-phenylpent-2-enoic Acid (2*E*). Synthesized according to method D using compound **2*E*a** (0.16 g, 0.51 mmol) and $NaOH_{aq}$ (1.1 mL, 5.1 mmol); white solid; yield: 0.105 g (72%); mp 117−118 °C. ^{1}H NMR ($CDCl_3$, 500 MHz): δ 2.70−2.74 (m, 2H), 3.37−3.41 (m, 2H), 6,11 (s, 1H), 7.12 (d, ^3J = 8.5 Hz, 2H), 7.22 (d, ^3J = 8.2 Hz, 2H), 7.39−7.42 (m, 3H), 7.44−7.48 (m, 2H). ^{13}C NMR ($CDCl_3$, 125 MHz): δ 17.2, 33.5, 60.2, 126.9, 127.6, 128.0, 128.1, 129.5, 131.2, 141.3, 144.8, 148.8, 180.5. NOESY experiment (^{1}H NMR ($CDCl_3$, 500 MHz) showed a cross peak between the signal at 7.44−7.48 (m, 2H) and the signal at 6.11 (s, 1H). LC/MS (+ESI): m/z 287.6 [MH$^+$], R_t = 14.13 (≥99%).

5.1.2.2. (*Z*)-5-(4-Chlorophenyl)-3-phenylpent-2-enoic Acid (2*Z*). Synthesized according to method D using compound **2*Z*a** (0.139 g, 0.44 mmol) and $NaOH_{aq}$ (1.1 mL, 4.4 mmol); white solid; yield: 0.093 g (74%); mp 114−115 °C. ^{1}H NMR ($CDCl_3$, 500 MHz): δ 2.64−2.67 (m, 2H), 2.71−2.77 (m, 2H), 5.87 (s, 1H), 7.04 (d, ^3J = 8.5 Hz, 2H), 7.18 (m, 2H), 7.24 (d, ^3J = 8.5 Hz, 2H), 7.34 (m, 3H). ^{13}C NMR ($CDCl_3$, 125 MHz): δ 15.9, 32.8, 60.2, 127.1, 127.6, 128.0, 129.7, 131.8, 139.8, 142.4, 145.3, 170.5. NOESY experiment (^{1}H NMR ($CDCl_3$, 500 MHz) showed a cross peak between the signals at 2.64−2.67 (m, 2H) and at 2.71−2.77 (m, 2H), and the signal at 5.87 (s, 1H). LC/MS (+ESI): m/z 287.5 [MH$^+$], R_t = 13.56 (≥99%).

5.1.2.3. (*Z*)-3-Phenyl-5-(4-(trifluoromethyl)phenyl)pent-2-enoic Acid (6*Z*). Synthesized according to method D using compound **6*Z*a** (0.15 g, 0.43 mmol) and $NaOH_{aq}$ (1.4 mL, 4.31 mmol); white solid; yield: 0.113 g (82%); mp 125−127 °C. ^{1}H NMR ($CDCl_3$, 500 MHz): δ 2.70−2.78 (m, 4H), 5.85 (s, 1H), 7.14−7.16 (m, 2H), 7.19−7.29 (m, 2H), 7.30−7.37 (m, 3H), 7.49−7.54 (m, 2H). ^{13}C NMR ($CDCl_3$, 125 MHz): δ 33.5, 34.9, 125.3 (d, J (C, F) = 3.7 Hz, CH), 125.9, 127.2, 127.5, 128.1, 128.5, 128.6, 128.8, 130.0, 133.5, 144.6, 160.6, 170.0. LC/MS (+ESI): m/z 321.5 [MH$^+$]; R_t = 13.74 (≥95%).

5.1.2.4. (*Z*)-5-(3,4-Dichlorophenyl)-3-phenylpent-2-enoic Acid (7*Z*). Synthesized according to method D using compound **7*Z*a** (0.10 g, 0.29 mmol) and $NaOH_{aq}$ (0.96 mL, 2.86 mmol); white solid; yield: 0.085 g (91%); mp 130−134 °C. ^{1}H NMR ($CDCl_3$, 500 MHz): δ 2.62−2.65 (m, 2H), 2.74−2.77 (m, 2H), 5.86 (s, 1H), 6.93 (dd, ^4J = 2.2, ^3J = 8.2 Hz, 2H), 7.16−7.21 (m, 2H), 7.31−7.39 (m, 4H). ^{13}C NMR ($CDCl_3$, 125 MHz): δ 32.5, 35.5, 116.8, 125.8, 126.9, 127.5, 127.9, 128.0, 128.2, 130.2, 133.3, 139.9, 140.4, 160.3, 169.9. LC/MS (+ESI): m/z 322.7 [MH$^+$]; R_t = 14.32 (≥99%).

5.1.2.5. (*Z*)-5-(2,4-Dichlorophenyl)-3-phenylpent-2-enoic Acid (8*Z*). Synthesized according to method D using compound **8*Z*a** (0.10 g, 0.31 mmol) and $NaOH_{aq}$ (0.32 mL, 0.93 mmol); white solid; yield: 0.09 g (87%); mp 122−124 °C. ^{1}H NMR ($CDCl_3$, 500 MHz): δ 2.67−2.74 (m, 4H), 5.88 (s, 1H), 7.03 (d, ^3J = 8.2 Hz, 1H), 7.14 (dd, ^3J = 2.2, ^4J = 8.2 Hz, 1H), 7.19−7.21 (m, 2H), 7.33−7.39 (m, 4H). ^{13}C NMR ($CDCl_3$, 125 MHz): δ 32.5, 40.2, 116.9, 127.1, 127.3, 128.2, 128.4, 129.4, 131.1, 132.7, 134.5, 138.7, 141.4, 160.5, 176.5. LC/MS (+ESI): *m*/*z* 322.7 [MH$^+$]; R_t = 14.63 (≥98%).

5.1.2.6. (*E*)-5-(Naphthalen-2-yl)-3-phenylpent-2-enoic Acid (12*E*). Synthesized according to method D using compound **12*E*a** (0.17 g, 0.51 mmol) and $NaOH_{aq}$ (1.70 mL, 5.14 mmol); white solid; yield: 0.143 g (93%); mp 147−150 °C. ^{1}H NMR ($CDCl_3$, 500 MHz): δ 2.91−2.94 (m, 2H), 3.49−3.53 (m, 2H), 6.14 (s, 1H), 7.38−7.44 (m, 6H), 7.51−7.53 (m, 2H), 7.62 (s, 1H), 7.74−7.79 (m, 3H). ^{13}C NMR ($CDCl_3$, 125 MHz): δ 33.3, 35.4, 116.5, 125.2, 126.5, 126.8, 127.2, 127.4, 127.9, 128.4, 128.7, 128.7, 129.4, 130.9, 132.1, 138.6, 138.7, 162.4, 170.9. LC/MS (+ESI): *m*/*z* 303.6 [MH$^+$]; R_t = 14.54 (≥99%).

5.1.2.7. (*Z*)-5-(Naphthalen-2-yl)-3-phenylpent-2-enoic Acid (12*Z*). Synthesized according to method D using compound **12*Z*a** (0.180 g, 0.54 mmol) and $NaOH_{aq}$ (1.80 mL, 5.45 mmol); white solid; yield: 0.150 g (92%); mp 117−120 °C. ^{1}H NMR ($CDCl_3$, 500 MHz): δ 2.84−2.89 (m, 4H), 5.92 (s, 1H), 7.21 (dd, ^4J = 1.7, ^3J = 8.2 Hz, 2H), 7.30−7.47 (m, 6H), 7.47−7.52 (m, 1H), 7.55 (s, 1H), 7.74−7.82 (m, 2H). ^{13}C NMR ($CDCl_3$, 125 MHz): δ 34.1, 42.5, 116.9, 125.6, 126.3, 126.7, 127.2, 127.5, 127.7, 127.9, 128.3, 128.4, 128.5, 128.7, 133.8, 138.3, 139.4, 159.8, 173.3. LC/MS (+ESI): *m*/*z* 303.5 [MH$^+$]; R_t = 14.02 (≥98%).

5.1.2.8. (*Z*)-5-(1*H*-Indol-3-yl)-3-phenylpent-2-enoic Acid (13*Z*). Synthesized according to method D using compound **13*Z*a** (0.20 g, 0.63 mmol) and $NaOH_{aq}$ (0.65 mL, 1.89 mmol); white solid; yield: 0.135 g (73%); mp 160−162 °C. ^{1}H NMR (CD_3OD, 500 MHz): δ 2.68−2.71 (m, 2H), 2.79−2.82 (m, 2H), 5.89 (s, 1H), 7.05 (t, ^3J = 7.9 Hz, 1H), 6.95 (dt, ^4J = 0.9, ^3J = 7.6 Hz, 1H), 7.05 (dt, ^4J = 0.9, ^3J = 7.6 Hz, 1H), 7.10−7.11 (d, ^4J = 2.2 Hz, 1H), 7.23−7.25 (m, 2H), 7.29−7.38 (m, 4H), 7.41 (d, ^3J = 7.9 Hz, 1H), 10.78 (s, NH), 11.85 (s, OH). ^{13}C NMR (CD_3OD, 125 MHz): δ 24.6, 42.3, 112.2, 115.1, 118.7, 119.2, 119.5, 122.3, 123.0, 128.5, 128.6, 128.7, 128.9, 138.2, 141.4, 160.7, 169.8. LC/MS (+ESI): *m*/*z* 292.5 [MH$^+$]; R_t = 11.93 (≥94%).

5.2. Biology. 5.2.1. Protein Kinases and Kinase Assays. All procedures were performed exactly as described previously.[22] In brief, PDK1 mutants were generated using site directed mutagenesis. Wild type and mutant protein kinases were expressed in HEK293 cells after transient transfection as GST fusion proteins and purified using glutathione sepharose. Cell-free protein kinase activity assays were performed using T308tide as a substrate peptide, and started using γ^{32}P-ATP. Phosphorylated peptides were spotted on P81 phosphocellulose paper (Whatman), washed by diluted phosphoric acid and incorporated ^{32}P quantified in a PhosphoImager.

5.2.2. Isothermal Titration Calorimetry. The association reactions of PDK1 with the *Z* isomers were quantified by isothermal titration calorimetry using the high precision VP-ITC titration calorimetric system (MicroCal Inc., MA) and protocols previously described.[41] Briefly, $PDK1_{50-359}$ and the compounds were dissolved in the same buffer (50 mM TrisHCl, pH 7.5, 200 mM NaCl, 1 mM DTT). The binding enthalpies were obtained by injecting the activators (450 μM) into the calorimetric cell containing the enzyme (20 μM). The solutions were thoroughly degassed under vacuum, and each experiment was performed at 20 °C by one injection of 2 μL followed by 29 injections of 10 μL with 210 s between injections using a 290 rpm rotating syringe. Heat signals were corrected for the heats of dilution and normalized to the amount of compound injected. Normalization and deconvolution of the binding isotherms was carried out using Origin7[42] provided by the manufacturer.

Acknowledgment. We thank Prof. Dr. S. Zeuzem for his generous support of the R.M.B. lab. We acknowledge the support by the Deutsche Forschungsgemeinschaft (BI 1044/2-2), by the Europrofession Foundation (Saarbrücken, Germany) to R.M.B. and M.E., by the Deutsche José Carreras Leukamie-Stiftung (DJCLS R 06/07) to M.E., and by the GoBio grant from the German Federal Ministry of Education and Science to R.M.B. and M.E.

Supporting Information Available: Synthetic procedures and NMR spectroscopic data of compounds **2c**−**14c**, **21c**, **2b**−**13b**, **15b**−**18b**, **21b**, **2a**−**20a**, **21*E*a**, **3**−**5*Z***, **9**−**11*Z***, **14**−**15*Z***, **18*Z***, **3**−**11*E***, **13**−**14*E***, **18*E***, **16**−**17*E*/*Z***, **19**, **20**, **21**; 2D-NOESY−^{1}H NMR spectroscopic data on **2*Z*/2*E***. This material is available free of charge via the Internet at http://pubs.acs.org.

References

(1) Cohen, P. Protein kinases—the major drug targets of the twenty-first century? *Nat Rev. Drug Discovery*. **2002**, *1*, 309–315.
(2) Mora, A.; Komander, D.; van Aalten, D. M.; Alessi, D. R. PDK1, the master regulator of AGC kinase signal transduction. *Semin. Cell. Dev. Biol*. **2004**, *15*, 161–170.
(3) Bayascas, J. R.; Leslie, N. R.; Parsons, R.; Fleming, S.; Alessi, D. R. Hypomorphic mutation of PDK1 suppresses tumorigenesis in PTEN(±) mice. *Curr. Biol*. **2005**, *15*, 1839–1846.
(4) Biondi, R. M.; Cheung, P. C.; Casamayor, A.; Deak, M.; Currie, R. A.; Alessi, D. R. Identification of a pocket in the PDK1 kinase domain that interacts with PIF and the C-terminal residues of PKA. *EMBO J*. **2000**, *19*, 979–988.
(5) Biondi, R. M.; Kieloch, A.; Currie, R. A.; Deak, M.; Alessi, D. R. The PIF-binding pocket in PDK1 is essential for activation of S6K and SGK but not PKB. *EMBO J*. **2001**, *20*, 4380–4390.
(6) Frodin, M.; Antal, T. L.; Dummler, B. A.; Jensen, C. J.; Deak, M.; Gammeltoft, S.; Biondi, R. M. A phosphoserine/threonine-binding pocket in AGC kinases and PDK1 mediates activation by hydrophobic motif phosphorylation. *EMBO J*. **2002**, *21*, 5396–5407.
(7) Biondi, R. M.; Komander, D.; Thomas, C. C.; Lizcano, J. M.; Deak, M.; Alessi, D. R.; van Aalten, D. M. High resolution crystal structure of the human PDK1 catalytic domain defines the regulatory phosphopeptide docking site. *EMBO J*. **2002**, *21*, 4219–4228.
(8) Balendran, A.; Biondi, R. M.; Cheung, P. C.; Casamayor, A.; Deak, M.; Alessi, D. R. A 3-phosphoinositide-dependent protein kinase-1 (PDK1) docking site is required for the phosphorylation of protein kinase Czeta (PKCzeta) and PKC-related kinase 2 by PDK1. *J. Biol. Chem*. **2000**, *275*, 20806–20813.
(9) Collins, B. J.; Deak, M.; Arthur, J. S.; Armit, L. J.; Alessi, D. R. In vivo role of the PIF-binding docking site of PDK1 defined by knock-in mutation. *EMBO J*. **2003**, *22*, 4202–4211.
(10) Feldman, R. I.; Wu, J. M.; Polokoff, M. A.; Kochanny, M. J.; Dinter, H.; Zhu, D.; Biroc, S. L.; Alicke, B.; Bryant, J.; Yuan, S.; Buckman, B. O.; Lentz, D.; Ferrer, M.; Whitlow, M.; Adler, M.; Finster, S.; Chang, Z.; Arnaiz, D. O. Novel small molecule inhibitors of 3-phosphoinositide-dependent kinase-1. *J. Biol. Chem*. **2005**, *280*, 19867–19874.
(11) Islam, I.; Bryant, J.; Chou, Y. L.; Kochanny, M. J.; Lee, W.; Phillips, G. B.; Yu, H.; Adler, M.; Whitlow, M.; Ho, E.; Lentz, D.; Polokoff, M. A.; Subramanyam, B.; Wu, J. M.; Zhu, D.; Feldman, R. I.; Arnaiz, D. O. Indolinone based phosphoinositide-dependent kinase-1 (PDK1) inhibitors. Part 1: design, synthesis and biological activity. *Bioorg. Med. Chem. Lett*. **2007**, *17*, 3814–3818.
(12) Sato, S.; Fujita, N.; Tsuruo, T. Interference with PDK1-Akt survival signaling pathway by UCN-01 (7-hydroxystaurosporine). *Oncogene* **2002**, *21*, 1727–1738.
(13) Stauffer, F.; Maira, S. M.; Furet, P.; Garcia-Echeverria, C. Imidazo[4,5-*c*]quinolines as inhibitors of the PI3K/PKB-pathway. *Bioorg. Med. Chem. Lett*. **2008**, *18*, 1027–1030.
(14) Peifer, C.; Alessi, D. R. Small-Molecule Inhibitors of PDK1. *ChemMedChem* **2008**, *3*, 1810–1838.
(15) Sausville, E. A.; Arbuck, S. G.; Messmann, R.; Headlee, D.; Bauer, K. S.; Lush, R. M.; Murgo, A.; Figg, W. D.; Lahusen, T.; Jaken, S.; Jing, X.; Roberge, M.; Fuse, E.; Kuwabara, T.; Senderowicz, A. M. Phase I trial of 72-h continuous infusion UCN-01 in patients with refractory neoplasms. *J. Clin. Oncol*. **2001**, *19*, 2319–2333.
(16) Welch, S.; Hirte, H. W.; Carey, M. S.; Hotte, S. J.; Tsao, M. S.; Brown, S.; Pond, G. R.; Dancey, J. E.; Oza, A. M. UCN-01 in combination with topotecan in patients with advanced recurrent

ovarian cancer: a study of the Princess Margaret Hospital Phase II consortium. *Gynecol. Oncol.* **2007**, *106*, 305–310.
(17) Edelman, M. J.; Bauer, K. S.Jr.; Wu, S.; Smith, R.; Bisacia, S.; Dancey, J. Phase I and pharmacokinetic study of 7-hydroxystaurosporine and carboplatin in advanced solid tumors. *Clin. Cancer. Res.* **2007**, *13*, 2667–2674.
(18) Kortmansky, J.; Shah, M. A.; Kaubisch, A.; Weyerbacher, A.; Yi, S.; Tong, W.; Sowers, R.; Gonen, M.; O'Reilly, E.; Kemeny, N.; Ilson, D. I.; Saltz, L. B.; Maki, R. G.; Kelsen, D. P.; Schwartz, G. K. Phase I trial of the cyclin-dependent kinase inhibitor and protein kinase C inhibitor 7-hydroxystaurosporine in combination with fluorouracil in patients with advanced solid tumors. *J. Clin. Oncol.* **2005**, *23*, 1875–1884.
(19) Davies, S. P.; Reddy, H.; Caivano, M.; Cohen, P. Specificity and mechanism of action of some commonly used protein kinase inhibitors. *Biochem. J.* **2000**, *351*, 95–105.
(20) Bain, J.; McLauchlan, H.; Elliott, M.; Cohen, P. The specificities of protein kinase inhibitors: an update. *Biochem. J.* **2003**, *371*, 199–204.
(21) Kiselyov, A.; Balakin, K. V.; Tkachenko, S. E.; Savchuk, N. P. Recent progress in development of non-ATP competitive small-molecule inhibitors of protein kinases. *Mini Rev. Med. Chem.* **2006**, *6*, 711–717.
(22) Engel, M.; Hindie, V.; Lopez-Garcia, L. A.; Stroba, A.; Schaeffer, F.; Adrian, I.; Imig, J.; Idrissova, L.; Nastainczyk, W.; Zeuzem, S.; Alzari, P. M.; Hartmann, R. W.; Piiper, A.; Biondi, R. M. Allosteric activation of the protein kinase PDK1 with low molecular weight compounds. *EMBO J.* **2006**, *25*, 5469–5480.
(23) Kishore, A. H.; Vedamurthy, B. M.; Mantelingu, K.; Agrawal, S.; Reddy, B. A.; Roy, S.; Rangappa, K. S.; Kundu, T. K. Specific small-molecule activator of Aurora kinase A induces autophosphorylation in a cell-free system. *J. Med. Chem.* **2008**, *51*, 792–797.
(24) Conn, P. J.; Christopoulos, A.; Lindsley, C. W. Allosteric modulators of GPCRs: a novel approach for the treatment of CNS disorders. *Nat. Rev. Drug Discovery* **2009**, *8*, 41–54.
(25) Hindie, V.; Stroba, A.; Zhang, H.; Lopez-Garcia, L. A.; Idrissova, L.; Zeuzem, S.; Hirschberg, D.; Schaeffer, F.; Jorgensen, T. J.; Engel, M.; Alzari, P. M.; Biondi, R. M. High resolution complex structure and allosteric effects of low molecular weight activators on the protein kinase PDK1. *Nat. Chem. Biol.* **2009**, DOI: 10.1038/nchembio.208.
(26) Yasui, S.; Fujii, M.; Ohno, A. NAD(P)$^+$−NAD(P)H Models. 64. The Quantitative Elucidation of the Mechanistic Aspects in the Silica Gel-Catalyzed Reduction of α,β-Unsaturated Carbonyl Compounds by a Model of NAD(P)H. *Bull. Chem. Soc. Jpn.* **1987**, *60*, 4019–4026.
(27) Yoshizawa, K.; Toyota, S.; Toda, F.; Csöregh, I. Preparative and mechanistic studies of solvent free Ra-Stoermer reactions. *Green Chem.* **2003**, *5*, 353–356.
(28) Beck, J. A. Direct Synthesis of Benzo[*b*]thiophene-2-carboxylate Esters involving Nitro Displacement. *J. Org. Chem.* **1972**, *37*, 3224–3226.
(29) Grover, J. R.; Walters, E. A.; Hui, E. T. Dissociation Energies of the Benzene Dimer and Dimer Cation. *J. Phys. Chem.* **1987**, *91*, 3233–3237.
(30) Laatikainen, R.; Ratilainen, J.; Sebastian, R.; Santa, H. NMR study of aromatic-aromatic interactions for benzene and some other fundamental aromatic systems using alignment of aromatics in strong magnetic field. *J. Am. Chem. Soc.* **1995**, *117*, 11006–11010.
(31) Nishio, M.; Umezawa, Y.; Hirota, M.; Takeuchi, Y. The CH/π interaction: significance in molecular recognition. *Tetrahedron* **1995**, *51*, 8665–8701.
(32) Gilli, P.; Ferretti, V.; Gilli, G.; Borea, P. A. Enthalpy−Entropy Compensation in Drug Receptor Binding. *J. Phys. Chem.* **1994**, *98*, 1515–1518.
(33) Grunwald, E.; Steel, C. Solvent Reorganization and Thermodynamic Enthalpy−Entropy Compensation. *J. Am. Chem. Soc.* **1995**, *117*, 5687–5692.
(34) Grunwald, E. Thermodynamics of Molecular Species; Wiley & Sons: New York, 1997.
(35) Velazquez-Campoy, A.; Luque, I.; Todd, M. J.; Milutinovich, M.; Kiso, Y.; Freire, E. Thermodynamic dissection of the binding energetics of KNI-272, a potent HIV-1 protease inhibitor. *Protein Sci.* **2000**, *9*, 1801–1809.
(36) Dunitz, J. D. Win some, lose some: enthalpy−entropy compensation in weak intermolecular interactions. *Chem. Biol.* **1995**, *2*, 709–712.
(37) Lafont, V.; Armstrong, A. A.; Ohtaka, H.; Kiso, Y.; Mario Amzel, L.; Freire, E. Compensating enthalpic and entropic changes hinder binding affinity optimization. *Chem. Biol. Drug Des.* **2007**, *69*, 413–422.
(38) Anderka, O.; Loenze, P.; Klabunde, T.; Dreyer, M. K.; Defossa, E.; Wendt, K. U.; Schmoll, D. Thermodynamic characterization of allosteric glycogen phosphorylase inhibitors. *Biochemistry* **2008**, *47*, 4683–4691.
(39) Ruben, A. J.; Kiso, Y.; Freire, E. Overcoming roadblocks in lead optimization: a thermodynamic perspective. *Chem. Biol. Drug Des.* **2006**, *67*, 2–4.
(40) Nezami, A.; Luque, I.; Kimura, T.; Kiso, Y.; Freire, E. Identification and characterization of allophenylnorstatine-based inhibitors of plasmepsin II, an antimalarial target. *Biochemistry* **2002**, *41*, 2273–2280.
(41) Schaeffer, F.; Matuschek, M.; Guglielmi, G.; Miras, I.; Alzari, P. M.; Beguin, P. Duplicated dockerin subdomains of *Clostridium thermocellum* endoglucanase CelD bind to a cohesin domain of the scaffolding protein CipA with distinct thermodynamic parameters and a negative cooperativity. *Biochemistry* **2002**, *41*, 2106–2114.
(42) Wiseman, T.; Williston, S.; Brandts, J. F.; Lin, L. N. Rapid measurement of binding constants and heats of binding using a new titration calorimeter. *Anal. Biochem.* **1989**, *179*, 131–137.